

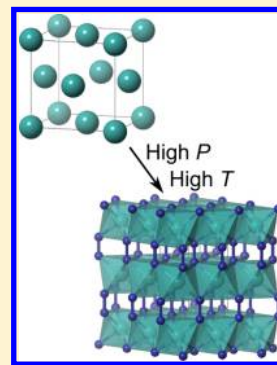
Direct Reaction between Copper and Nitrogen at High Pressures and Temperatures

Jack Binns,[†] Mary-Ellen Donnelly,[†] Miriam Peña-Alvarez,^{‡,§} Mengnan Wang,[†] Eugene Gregoryanz,^{†,‡} Andreas Hermann,^{‡,§} Philip Dalladay-Simpson,[†] and Ross T. Howie^{*,†}

[†]Center for High Pressure Science and Technology Advanced Research (HPSTAR), Shanghai 201203, China

[‡]Centre for Science at Extreme Conditions and The School of Physics & Astronomy, The University of Edinburgh, Peter Guthrie Tait Road, Edinburgh EH9 3FD, United Kingdom

ABSTRACT: Transition-metal nitrides have applications in a range of technological fields. Recent experiments have shown that new nitrogen-bearing compounds can be accessed through a combination of high temperatures and pressures, revealing a richer chemistry than was previously assumed. Here, we show that at pressures above 50 GPa and temperatures greater than 1500 K elemental copper reacts with nitrogen, forming copper diazenide (CuN₂). Through a combination of synchrotron X-ray diffraction and first-principles calculations we have explored the stability and electronic structure of CuN₂. We find that the novel compound remains stable down to 25 GPa before decomposing to its constituent elements. Electronic structure calculations show that CuN₂ is metallic and exhibits partially filled N₂ antibonding orbitals, leading to an ambiguous electronic structure between Cu⁺/Cu²⁺. This leads to weak Cu–N bonds and the lowest bulk modulus observed for any transition-metal nitride.



Nitrogen is largely inert under atmospheric conditions; however, it forms a large number of technologically important materials with main group elements and transition metals. Nitride compounds have been an important focus of inorganic chemistry for many decades and are typically synthesized at high temperatures.¹ Recently, alternative high-pressure synthesis methods have proven highly successful for the discovery of novel materials which have been proposed as ideal candidates in a range of areas from high bulk modulus materials^{2–4} to explosives.^{5,6}

Solids with polymeric networks of N–N single bonds^{7,8} should act as excellent high energy density materials if suitable synthesis routes can be found. Extensive theoretical work has predicted the existence of polynitride species for at least 16 metals (e.g., see refs 9–14), and recent experiments have begun to test these predictions, uncovering intriguing structures containing polymeric nitrogen chains,¹⁵ molecular inclusion compounds,¹⁶ and pentazolate anions,^{17,18} all synthesized under high-pressure and high-temperature reaction conditions.

The platinum-group metals (Pt,² Pd,⁴ Rh,¹⁹ Os,³ Ir,^{3,20} and Ru²¹) have been shown to form highly incompressible N-containing species. Although they crystallize in a range of different structures, these compounds share a number of features leading to high bulk moduli primarily N–N single bonds (≈ 1.4 Å) linking octahedrally coordinated N atoms.²² Numerous subsequent experimental and theoretical studies have continued to search for ultrahard materials among other transition-metal nitrides at high pressure.^{9,11,23–25}

The coinage metals (group 11: Cu, Ag, and Au) have so far shown a limited propensity to form nitrogen-bearing

compounds despite intense efforts utilizing an array of synthesis techniques including nitrogen-ion irradiation.^{26–29} Copper is known to form two nitrogen-containing compounds: copper azide (CuN₃), a highly sensitive explosive,³⁰ and copper nitride (Cu₃N), a stable semiconductor finding applications in a wide range of areas from lithium-ion battery electrodes to conductive ink and solar energy harvesting.^{31–33} Under compression, the narrow band gap (0.6 eV) of Cu₃N closes by ≈ 5 GPa, and no structural phase transitions are observed up to 26.7 GPa.³⁴ Silver also forms an explosive azide (AgN₃),³⁵ and attempts at forming stable gold nitrides have been limited to ion-irradiated surfaces.^{26,28}

Here, using a combination of high pressure and high temperatures, we have explored the synthesis of novel copper–nitrogen compounds. After laser heating at 50 GPa, we observe the direct reaction between copper and nitrogen forming a previously unknown copper diazenide with stoichiometry CuN₂. This compound is stable on decompression down to 25 GPa before decomposing to its constituent elements. Calculations show CuN₂ is a metal with a copper oxidation state lying between +1 and +2. As a result, CuN₂ contains highly compressible Cu–N bonds giving mechanical properties far more in common with alkaline earth diazenides^{36–38} than other transition-metal nitrides.

Samples of Cu powder were compressed in solid N₂ and laser heated at 10 GPa intervals up to 50 GPa with no observed changes in diffraction patterns with the exception of the known

Received: January 9, 2019

Accepted: February 20, 2019

Published: February 20, 2019

phase transitions in pure N_2 .^{39,40} Above 52 GPa, the Cu sample coupled strongly, with temperatures in excess of ~ 1500 K. Upon quenching, numerous new diffraction lines appeared (Figure 1a), all of which could be indexed to a hexagonal unit

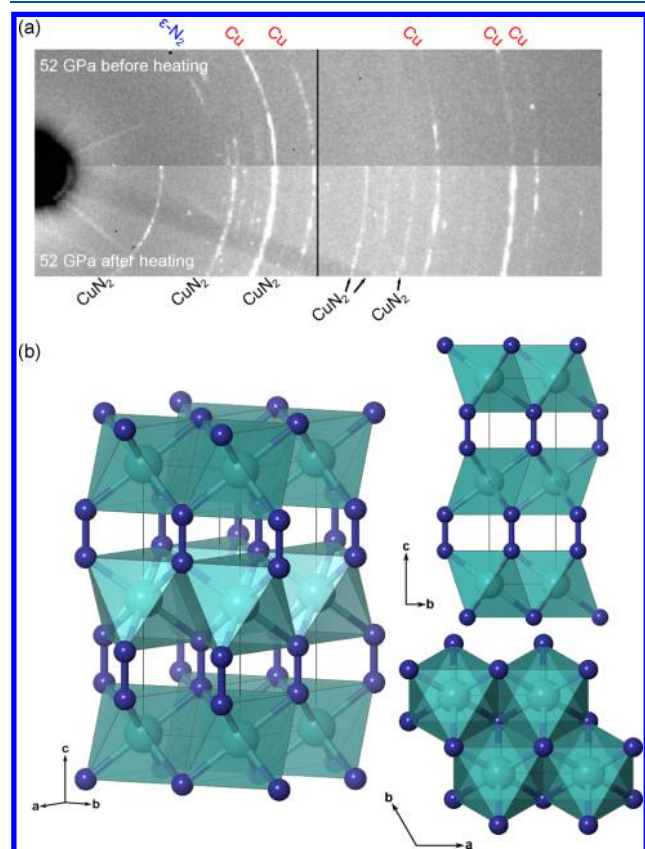


Figure 1. High pressure X-ray diffraction patterns ($\lambda = 0.3344$ Å) showing (a) the synthesis of CuN_2 by laser heating at 52 GPa. (b) Crystal structure of CuN_2 . Cu atoms are green, and N atoms blue. Optimized structural parameters derived from DFT calculations at 52 GPa: $a = 2.741$, $c = 7.0417$ Å, $Cu[2a(0, 0, 0)]$, $N[4f(\frac{1}{3}, \frac{2}{3}, 0.6650)]$.

cell [$a = 2.6759(5)$, $c = 7.235(3)$ Å, at 52 GPa] (Figure 2), with systematic absences indicating the presence of a c -glide normal to $[1\bar{1}1]$. Attempts to solve the crystal structure were hindered by numerous overlapping reflections from $\epsilon-N_2$; however, a possible solution was found by direct methods in space group $P6_3/mmc$,⁴¹ with stoichiometry CuN_2 . Rietveld refinement required excluding regions of the profile which overlapped with peaks due to $\epsilon-N_2$ because diffraction from $\epsilon-N_2$ took the form of quasi-single-crystal diffraction peaks unsuitable for inclusion in the refinement. Because of the poor quality of the data, the nitrogen-atom position was poorly defined, giving a large uncertainty on the experimentally determined N–N bond distance (1.3(3) Å). However, despite extensive overlapping, unit-cell dimensions of this new phase could be extracted (Figure 3b), and the resulting changes in unit-cell volume with pressure (Figure 3a) also suggest a stoichiometry of CuN_2 . To confirm our experimental structural analysis and to explore the electronic structure of CuN_2 , we have performed density functional theory (DFT) geometry optimization calculations. We find that the structure converges to close agreement with experimentally determined unit-cell dimensions (Figure 3b).

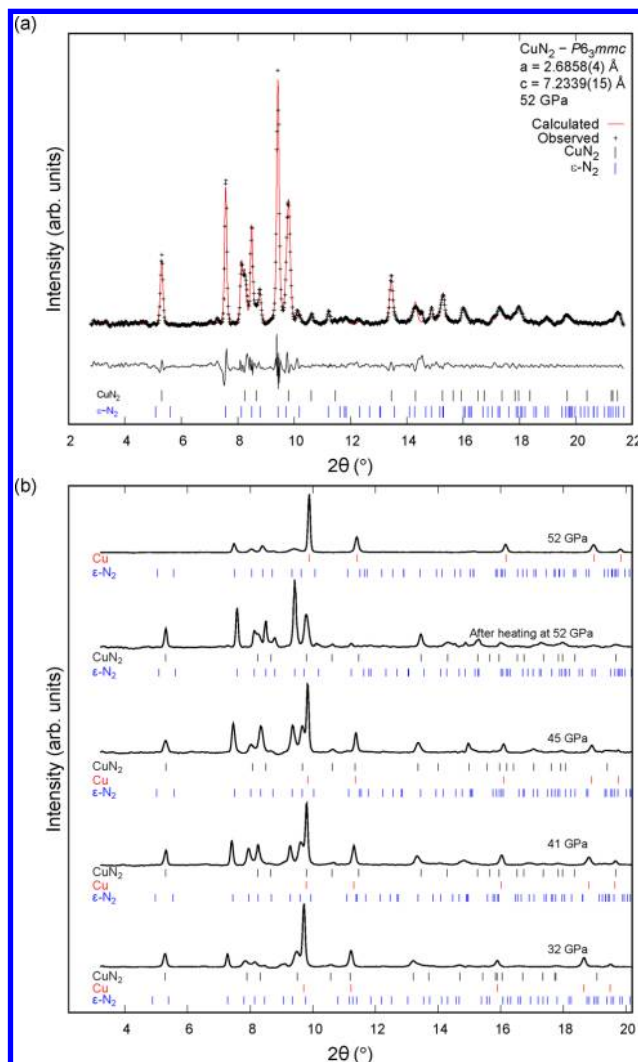


Figure 2. (a) Representative Le Bail refinement of CuN_2 data at 52 GPa $wR_p = 0.39$ ($\lambda = 0.3344$ Å). (b) Synthesis and decompression of CuN_2 . Tick marks indicate Bragg reflection positions for the noted phase.

The optimized structure of the novel compound CuN_2 contains octahedrally coordinated Cu atoms, in common with many transition-metal–nitrogen compounds (e.g., PtN_2 ² and FeN_2 ¹⁵). These edge-sharing CuN_6 octahedra are arranged in layers in the ab -plane and are linked by N_2 anions aligned along the c -axis, with a N–N interatomic distance of 1.197 Å at 52 GPa. (Figure 1b). This N–N distance gives a direct insight into the nature of the electronic structure of transition-metal nitrides. In cases with high metal oxidation states, the transfer of electron density from the metal results in “pernitride” anions ($[N-N]^{4-}$) which form strong M–N bonds, have high bulk moduli, and show internal N–N distances of approximately 1.4 Å, seen in the archetypal examples of PtN_2 ,² OsN_2 ,³ and TiN_2 .²⁴ If the metal is limited to an oxidation state of +2, “diazene” ($[N=N]^{2-}$) anions are formed instead. In these compounds M–N bonding is weaker, bulk moduli are lower, and the internal N–N distances are shorter (≈ 1.2 Å). This is the case for the alkaline earth metal diazenides, BaN_2 and SrN_2 .⁴² The short N–N distance in CuN_2 (1.197 Å) would appear to suggest that, by analogy, in this compound Cu is present as Cu^{2+} and is bonded to $[N=N]^{2-}$ anions. However, a Cu^{2+} ion would be expected to display a Jahn–Teller

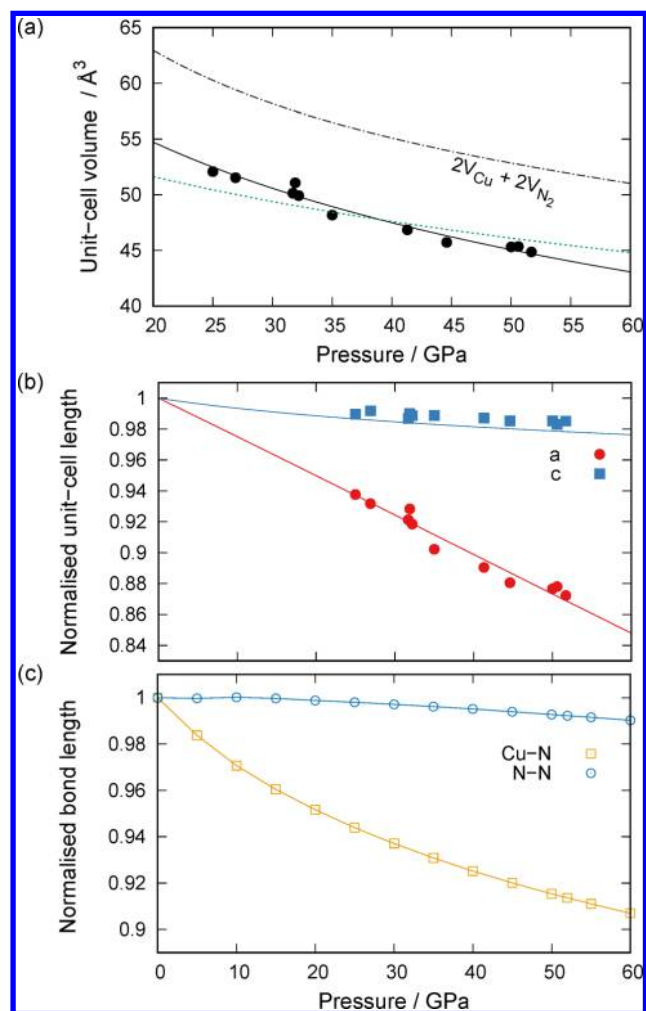


Figure 3. (a) Change in CuN₂ unit-cell volume with pressure. Dashed line indicates volume of pure Cu + N₂ for comparison. The solid line indicates fitted Vinet equation of state ($V_0 = 62.3(13) \text{ \AA}^3$, $K_0 = 130(11) \text{ GPa}$, $K' = 1$), and the dotted line shows the unit-cell volume derived from DFT calculations. (b) Changes in normalized unit-cell lengths for CuN₂. a_0 and c_0 are derived from calculations. (c) Changes in normalized bond lengths for Cu–N (yellow squares) and N–N (blue circles) with pressure.

distortion, which is not consistent with the proposed crystal structure. To understand this discrepancy, lattice dynamics calculations were carried out at 0 and 50 GPa, and at both pressures the $P6_3/mmc$ structure is dynamically stable and all phonons are real, indicating the absence of a driving force to distort the CuN₆ octahedra. Furthermore, geometry optimization of a distorted structure in the orthorhombic subgroup $Cmcm$ resulted in a return to $P6_3/mmc$ symmetry within numerical accuracy.

A more detailed understanding of the electronic structure of CuN₂ is gained through the crystal orbital Hamiltonian population (COHP) analysis.^{43,44} The electronic density of states of CuN₂ is shown in Figure 4a. This shows CuN₂ to be a metal with no clear character to the states at the Fermi level, but it is dominated by Cu-3d and N-2p states as expected. The N-2p states are antibonding in character (Figure 4b): the partial -COHP(N–N) is negative around the Fermi level. There is a gap at 4 eV above the Fermi level corresponding to the filling of additional N₂ $1\pi_g^*$ and $2\sigma_u^*$ states. A more quantitative picture arises from the integration of the

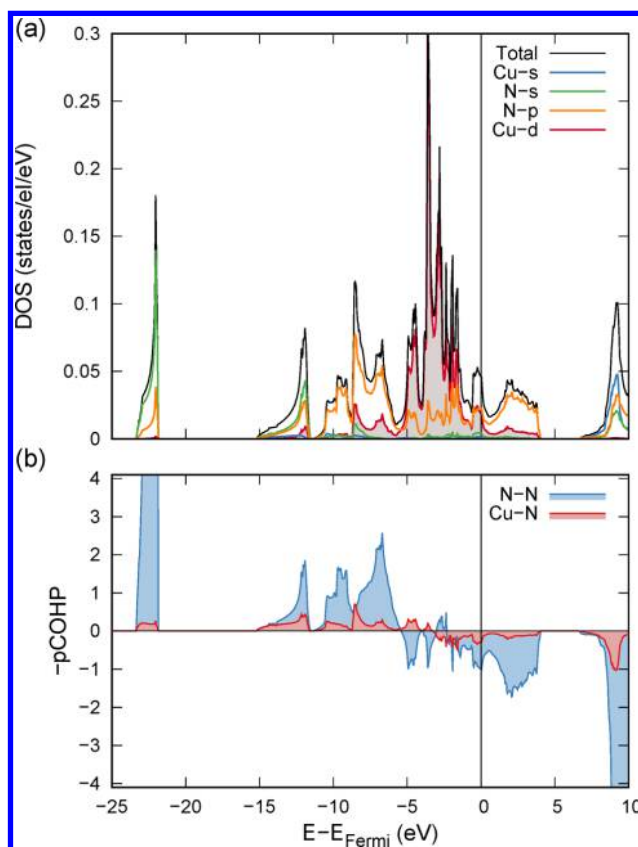


Figure 4. (a) Electronic density of states and (b) COHP analysis of CuN₂ at 50 GPa.

COHP(N–N) over the energy range of these antibonding orbitals from -5 to 5 eV, as seen in Figure 4b. The resulting 32.5% occupancy is significantly less than the 50% expected for $[\text{N}=\text{N}]^{2-}$ anions³⁸ and, combined with the absence of a Jahn–Teller distortion, intriguingly supports an ambivalent electronic state between $[\text{N}=\text{N}]^-$ and $[\text{N}=\text{N}]^{2-}$.

From the synthesis pressure, samples were decompressed to determine the stability of this newly synthesized copper diazenide. Below 25 GPa, peaks due to CuN₂ disappear, leaving only those from Cu and ϵ -N₂. Changes in unit-cell volume with pressure were fitted with a Vinet equation of state, giving a bulk modulus of $K_0(\text{CuN}_2) = 130(11) \text{ GPa}$, extremely close to that of Cu (140 GPa) and comparable to the low bulk moduli observed for the alkaline earth metal diazenides [$K_0(\text{BaN}_2) = 46 \text{ GPa}$, $K_0(\text{SrN}_2) = 65 \text{ GPa}$].⁴² Unsurprisingly then, the overall compressibility appears very similar to that calculated from the pure elements (Figure 3a).

Closer analysis shows the majority of this compression is taken up by the a and b axes; by 52 GPa, the a -axis decreases by 12.8% ($-0.392(5) \text{ \AA}$) relative to the calculated ambient pressure value as compared to the far more rigid c axis, which decreases by just 0.65% ($-0.047(3) \text{ \AA}$) over the same pressure range (Figure 3b). The origin of this anisotropic behavior lies in the contrasting strengths of Cu–N and N–N bonding, as shown in Figure 3c. As would be expected for a strongly bonded diazenide anion, the N=N distance reduces by less than 1% up to 60 GPa, almost an order of magnitude more resilient than the Cu–N bonds which compress by -9.3% . The presence of the highly compressible M–N bond and the resulting low bulk modulus again marks CuN₂ as being far more similar to the alkaline earth diazenides than other

transition-metal nitrides. This is the logical conclusion to the trend observed across the first-row transition-metal nitrides MN_2 ; as the N_2 anion shows greater molecular character, $M-N$ bonds weaken and bulk moduli reduce: $K_0(TiN_2) = 382(3)$ GPa,²⁴ $K_0(FeN_2) = 344(13)$ GPa,²⁵ $K_0(CoN_2) = 216(18)$ GPa,⁴⁵ and $K_0(CuN_2) = 130(11)$ GPa.

In conclusion, we have utilized in situ laser heating combined with high pressures to perform the first direct reaction between elemental nitrogen and a coinage metal to form a novel copper diazenide (CuN_2) compound. The structure was determined by a combination of powder X-ray diffraction and DFT calculations. Surprisingly for a transition-metal nitride, CuN_2 is highly compressible because of the presence of extremely weak $Cu-N$ bonds. The origins of this surprising behavior lie in the limited electron transfer between Cu and N_2 . Electronic structure analysis indicates partially filled antibonding orbitals on the N_2 anions which combined with the absence of a Jahn–Teller distortion, suggests an electronic structure between $Cu^+[N=N]^-$ and $Cu^{2+}[N=N]^{2-}$. This compound remains stable down to 25 GPa before decomposing to its constituent elements.

EXPERIMENTAL SECTION

High-purity copper powder (99.8%, 1.6 μm particle size) from Alfa Aesar was placed into diamond-anvil cells (DAC) and subsequently loaded with high-purity nitrogen gas (99.9%) at 0.17 GPa. Loading of nitrogen was confirmed by the observation of the nitrogen vibrational mode using a custom-built microfocused Raman system.⁴⁶ Rhenium gaskets were used to form the sample chamber in all experimental runs with diamond-anvil culets ranging from 200 to 300 μm .

The Cu sample was heated in situ from both sides uniaxially by directly coupling to an yttrium–aluminum–garnet (YAG) laser with wavelength $\lambda = 1064$ nm. Angle-dispersive X-ray diffraction data were collected at beamline 13-IDD (GSECARS) at APS, United States.⁴⁷ The diffraction from 0.3344 Å wavelength X-rays was recorded using a Pilatus 1 M image-plate detector. Two-dimensional image-plate data were integrated with *DIOPTAS* to yield intensity versus 2θ plots.⁴⁸ Diffraction patterns were indexed with *CONOGRAPH*,⁴⁹ Le Bail and Rietveld refinement was carried out in *Jana2006*.^{50–52}

Total energy calculations were carried out within the framework of DFT in conjunction with the projector-augmented wave method and a plane wave basis, as implemented in the VASP code.^{53,54} We used the PBE exchange–correlation functional⁵⁵ and included the Cu 3p, 4s, and 3d and N 2s and 2p electrons in the valence space. Brillouin zone sampling was done on regular k -point grids with linear densities of $50/\text{\AA}^{-1}$; the plane wave cutoff energy was 1000 eV. Structures were optimized over a sequence of pressures until remaining forces on the atoms were smaller than 1 meV/Å. Partial DOS and COHP analyses were carried out using *LOBSTER*.⁵⁶

AUTHOR INFORMATION

Corresponding Author

*E-mail: ross.howie@hpstar.ac.cn.

ORCID

Jack Binns: 0000-0001-5421-6841

Miriam Peña-Alvarez: 0000-0001-7056-7158

Andreas Hermann: 0000-0002-8971-3933

Notes

The authors declare no competing financial interest.

ACKNOWLEDGMENTS

This work were performed at GeoSoilEnviroCARS (The University of Chicago, Sector 13), Advanced Photon Source (APS), Argonne National Laboratory. GeoSoilEnviroCARS is supported by the National Science Foundation–Earth Sciences (No. EAR-1634415) and Department of Energy–GeoSciences (No. DE-FG02-94ER14466). This research used resources of the Advanced Photon Source, a U.S. Department of Energy (DOE) Office of Science User Facility operated for the DOE Office of Science by Argonne National Laboratory under Contract No. DE-AC02-06CH11357. M.P.-A. acknowledges the support of the European Research Council (ERC) Grant Hecate Reference No. 695527 secured by Graeme J. Ackland. Computational resources provided by the UK's National Supercomputer Service through the UK Car–Parrinello consortium (EPSRC Grant No. EP/P022561/1) and by the UK Materials and Molecular Modelling Hub (No. EP/P020194) are gratefully acknowledged. Funding has been provided by the respective Chinese “1000 Talent Award” grants of both P.D.-S. and R.T.H. We also thank the referees for their helpful comments.

REFERENCES

- (1) Höhn, P.; Niewa, R. In *Handbook of Solid State Chemistry*; Dronskowski, R., Kikkawa, S., Stein, A., Eds.; Wiley-VCH, 2017; Chapter 7, pp 251–361.
- (2) Gregoryanz, E.; Sanloup, C.; Somayazulu, M.; Badro, J.; Fiquet, G.; Mao, H.-k.; Hemley, R. J. Synthesis and Characterization of a Binary Noble Metal Nitride. *Nat. Mater.* **2004**, *3*, 294–297.
- (3) Young, A. F.; Sanloup, C.; Gregoryanz, E.; Scandolo, S.; Hemley, R. J.; Mao, H. K. Synthesis of Novel Transition Metal Nitrides IrN_2 and OsN_2 . *Phys. Rev. Lett.* **2006**, *96*, 155501.
- (4) Crowhurst, J. C.; Crowhurst, J. C.; Goncharov, A. F.; Sadigh, B.; Evans, C. L.; Morrall, P. G.; Ferreira, J. L.; Nelson, A. J. Synthesis and Characterization of the Nitrides of Platinum and Iridium. *Science* **2006**, *311*, 1275–1278.
- (5) Pickard, C. J.; Needs, R. J. High-Pressure Phases of Nitrogen. *Phys. Rev. Lett.* **2009**, *102*, 125702.
- (6) Li, Y. C.; Qi, C.; Li, S. H.; Zhang, H. J.; Sun, C. H.; Yu, Y. Z.; Pang, S. P. 1,1'-Azobis1,2,3-triazole: A high-nitrogen compound with stable N_8 Structure and Photochromism. *J. Am. Chem. Soc.* **2010**, *132*, 12172–12173.
- (7) Eremets, M. I.; Gavriluk, A. G.; Trojan, I. A.; Dzivenko, D. A.; Boehler, R. Singlebonded cubic form of nitrogen. *Nat. Mater.* **2004**, *3*, 558–563.
- (8) Gregoryanz, E.; Goncharov, A. F.; Sanloup, C.; Somayazulu, M.; Mao, H.-k.; Hemley, R. J. High P-T transformations of nitrogen to 170 GPa. *J. Chem. Phys.* **2007**, *126*, 184505.
- (9) Aydin, S.; Ciftci, Y. O.; Tatar, A. Superhard transition metal tetranitrides: XN_4 ($X = Re, Os, W$). *J. Mater. Res.* **2012**, *27*, 1705–1715.
- (10) Prasad, D. L.; Ashcroft, N. W.; Hoffmann, R. Evolving structural diversity and metallicity in compressed lithium azide. *J. Phys. Chem. C* **2013**, *117*, 20838–20846.
- (11) Zhao, Z.; Bao, K.; Li, D.; Duan, D.; Tian, F.; Jin, X.; Chen, C.; Huang, X.; Liu, B.; Cui, T. Nitrogen concentration driving the hardness of rhenium nitrides. *Sci. Rep.* **2015**, *4*, 4797.
- (12) Zhu, S.; Peng, F.; Liu, H.; Majumdar, A.; Gao, T.; Yao, Y. Stable Calcium Nitrides at Ambient and High Pressures. *Inorg. Chem.* **2016**, *55*, 7550–7555.
- (13) Zhang, J.; Oganov, A. R.; Li, X.; Niu, H. Pressure-stabilized hafnium nitrides and their properties. *Phys. Rev. B: Condens. Matter Mater. Phys.* **2017**, *95*, No. 020103.

- (14) Kvashnin, A. G.; Oganov, A. R.; Samtsevich, A. I.; Allahyari, Z. Computational Search for Novel Hard Chromium-Based Materials. *J. Phys. Chem. Lett.* **2017**, *8*, 755–764.
- (15) Bykov, M.; Bykova, E.; Aprilis, G.; Glazyrin, K.; Koemets, E.; Chuvashova, I.; Kupenko, I.; McCammon, C.; Mezouar, M.; Prakapenka, V.; et al. Fe-N system at high pressure reveals a compound featuring polymeric nitrogen chains. *Nat. Commun.* **2018**, *9*, 2756.
- (16) Bykov, M.; Bykova, E.; Koemets, E.; Fedotenko, T.; Aprilis, G.; Glazyrin, K.; Liermann, H. P.; Ponomareva, A. V.; Tidholm, J.; Tasnádi, F.; et al. High-Pressure Synthesis of a Nitrogen-Rich Inclusion Compound $\text{ReN}_8 \cdot x\text{N}_2$ with Conjugated Polymeric Nitrogen Chains. *Angew. Chem., Int. Ed.* **2018**, *57*, 9048–9053.
- (17) Laniel, D.; Weck, G.; Loubeyre, P. Direct Reaction of Nitrogen and Lithium up to 75 GPa: Synthesis of the Li_3N , LiN , LiN_2 , and LiN_5 Compounds. *Inorg. Chem.* **2018**, *57*, 10685–10693.
- (18) Steele, B. A.; Stavrou, E.; Crowhurst, J. C.; Zaug, J. M.; Prakapenka, V. B.; Oleynik, I. I. High-Pressure Synthesis of a Pentazolate Salt. *Chem. Mater.* **2017**, *29*, 735–741.
- (19) Niwa, K.; Dzivenko, D.; Suzuki, K.; Riedel, R.; Troyan, I.; Eremets, M.; Hasegawa, M. High Pressure Synthesis of Marcasite-Type Rhodium Pernitride. *Inorg. Chem.* **2014**, *53*, 697–699.
- (20) Crowhurst, J. C.; Goncharov, A. F.; Sadigh, B.; Zaug, J.; Aberg, D.; Meng, Y.; Prakapenka, V. B. Synthesis and characterization of nitrides of iridium and palladium. *J. Mater. Res.* **2008**, *23*, 1–5.
- (21) Niwa, K.; Suzuki, K.; Muto, S.; Tatsumi, K.; Soda, K.; Kikegawa, T.; Hasegawa, M. Discovery of the Last Remaining Binary Platinum-Group Pernitride. *Chem. - Eur. J.* **2014**, *20*, 13885–13888.
- (22) Liu, Z.; Gall, D.; Khare, S. Electronic and bonding analysis of hardness in pyrite-type transition-metal pernitrides. *Phys. Rev. B: Condens. Matter Mater. Phys.* **2014**, *90*, 134102.
- (23) Wessel, M.; Dronskowski, R. A New Phase in the Binary Iron Nitrogen System? - The Prediction of Iron Pernitride, FeN_2 . *Chem. - Eur. J.* **2011**, *17*, 2598–2603.
- (24) Bhadrani, V. S.; Kim, D. Y.; Strobel, T. A. High-Pressure Synthesis and Characterization of Incompressible Titanium Pernitride. *Chem. Mater.* **2016**, *28*, 1616–1620.
- (25) Laniel, D.; Dewaele, A.; Garbarino, G. High Pressure and High Temperature Synthesis of the Iron Pernitride FeN_2 . *Inorg. Chem.* **2018**, *57*, 6245.
- (26) Krishnamurthy, S.; Montalti, M.; Wardle, M.; Shaw, M.; Briddon, P.; Svensson, K.; Hunt, M.; Siller, L. Nitrogen ion irradiation of Au (110): Photoemission spectroscopy and possible crystal structures of gold nitride. *Phys. Rev. B: Condens. Matter Mater. Phys.* **2004**, *70*, No. 045414.
- (27) Tibbetts, G. G.; Burkstrand, J. M.; Tracy, J. C. Electronic properties of adsorbed layers of nitrogen, oxygen, and sulfur on copper (100). *Phys. Rev. B* **1977**, *15*, 3652–3660.
- (28) Siller, L.; Hunt, M. R. C.; Brown, J. W.; Coquel, J. M.; Rudolf, P. Nitrogen ion irradiation of Au(110): formation of gold nitride. *Surf. Sci.* **2002**, *513*, 78–82.
- (29) Lancaster, G. M.; Rabalais, J. W. Chemical Reactions of N^{2+} Ion Beams with First-Row Transition Metals. *J. Phys. Chem.* **1979**, *83*, 209–212.
- (30) Liu, X.; George, J.; Maintz, S.; Dronskowski, R. $\beta\text{-CuN}_3$: The overlooked ground-state polymorph of copper azide with heterographene-like layers. *Angew. Chem., Int. Ed.* **2015**, *54*, 1954–1959.
- (31) Wang, J.; Li, F.; Liu, X.; Zhou, H.; Shao, X.; Qu, Y.; Zhao, M. Cu_3N and its analogs: a new class of electrodes for lithium ion batteries. *J. Mater. Chem. A* **2017**, *5*, 8762–8768.
- (32) Nakamura, T.; Hayashi, H.; Hanaoka, T. A.; Ebina, T. Preparation of copper nitride (Cu_3N) nanoparticles in long-chain alcohols at 130–200 C and nitridation mechanism. *Inorg. Chem.* **2014**, *53*, 710–715.
- (33) Zakutayev, A.; Caskey, C. M.; Fioretti, A. N.; Ginley, D. S.; Vidal, J.; Stevanovic, V.; Tea, E.; Lany, S. Defect tolerant semiconductors for solar energy conversion. *J. Phys. Chem. Lett.* **2014**, *5*, 1117–1125.
- (34) Kuzmin, A.; Anspoks, A.; Kalinko, A.; Timoshenko, J.; Nataf, L.; Baudelet, F.; Irifune, T. Origin of Pressure-Induced Metallization in Cu_3N : An X-ray Absorption Spectroscopy Study. *Phys. Status Solidi B* **2018**, *255*, 1800073.
- (35) Schmidt, C. L.; Dinnebier, R.; Wedig, U.; Jansen, M. Crystal structure and chemical bonding of the high-temperature phase of AgN_3 . *Inorg. Chem.* **2007**, *46*, 907–916.
- (36) Vajenine, G. V.; Auffermann, G.; Prots, Y.; Schnelle, W.; Kremer, R. K.; Simon, A.; Kniep, R. Preparation, Crystal Structure, and Properties of Barium Pernitride, BaN_2 . *Inorg. Chem.* **2001**, *40*, 4866–4870.
- (37) Auffermann, G.; Prots, Y.; Kniep, R. SrN and SrN_2 : Diazenides by Synthesis under High N_2 -pressure. *Angew. Chem., Int. Ed.* **2001**, *40*, 547–549.
- (38) Schneider, S. B.; Seibald, M.; Deringer, V. L.; Stoffel, R. P.; Frankovsky, R.; Friederichs, G. M.; Laqua, H.; Duppel, V.; Jeschke, G.; Dronskowski, R.; et al. High-Pressure Synthesis and Characterization of $\text{Li}_2\text{Ca}_3[\text{N}_2]_3$ an Uncommon Metallic Diazenide with $[\text{N}_2]^{2-}$ Ions. *J. Am. Chem. Soc.* **2013**, *135*, 16668–16679.
- (39) Hanfland, M.; Lorenzen, M.; Wassilew-Reul, C.; Zontone, F. Structures of Molecular Nitrogen at High Pressures. *Koatsuryoku no Kagaku to Gijutsu* **1998**, *7*, 787–789.
- (40) Stinton, G.; Loa, L.; Lundegaard, L.; McMahon, M. The crystal structures of δ and δ^* nitrogen. *J. Chem. Phys.* **2009**, *131*, 104511.
- (41) Altomare, A.; Cuocci, C.; Giacovazzo, C.; Moliterni, A.; Rizzi, R.; Corriero, N.; Falcicchio, A. EXPO2013: a kit of tools for phasing crystal structures from powder data. *J. Appl. Crystallogr.* **2013**, *46*, 1231–1235.
- (42) Wessel, M.; Dronskowski, R. Nature of N-N Bonding within High-Pressure Noble-Metal Pernitrides and the Prediction of Lanthanum Pernitride. *J. Am. Chem. Soc.* **2010**, *132*, 2421–2429.
- (43) Dronskowski, R.; Bloechl, P. E. Crystal orbital Hamilton populations (COHP): energyresolved visualization of chemical bonding in solids based on density-functional calculations. *J. Phys. Chem.* **1993**, *97*, 8617–8624.
- (44) Maintz, S.; Deringer, V. L.; Tchougréeff, A. L.; Dronskowski, R. Analytic projection from plane-wave and PAW wavefunctions and application to chemical-bonding analysis in solids. *J. Comput. Chem.* **2013**, *34*, 2557–2567.
- (45) Niwa, K.; Terabe, T.; Kato, D.; Takayama, S.; Kato, M.; Soda, K.; Hasegawa, M. Highly Coordinated Iron and Cobalt Nitrides Synthesized at High Pressures and High Temperatures. *Inorg. Chem.* **2017**, *56*, 6410–6418.
- (46) Dalladay-Simpson, P.; Howie, R. T.; Gregoryanz, E. Evidence for a new phase of dense hydrogen above 325 gigapascals. *Nature* **2016**, *529*, 63–67.
- (47) Shen, G.; Prakapenka, V. B.; Eng, P. J.; Rivers, M. L.; Sutton, S. R. Facilities for high-pressure research with the diamond anvil cell at GSECARS. *J. Synchrotron Radiat.* **2005**, *12*, 642–649.
- (48) Prescher, C.; Prakapenka, V. B. DIOPTAS: a program for reduction of two-dimensional X-ray diffraction data and data exploration. *High Pressure Res.* **2015**, *35*, 223–230.
- (49) Oishi-Tomiyasu, R. Robust powder auto-indexing using many peaks. *J. Appl. Crystallogr.* **2014**, *47*, 593–598.
- (50) Le Bail, A.; Duroy, H.; Fourquet, J. Ab-initio structure determination of LiSbWO_6 by X-ray powder diffraction. *Mater. Res. Bull.* **1988**, *23*, 447–452.
- (51) Rietveld, H. M. A profile refinement method for nuclear and magnetic structures. *J. Appl. Crystallogr.* **1969**, *2*, 65–71.
- (52) Petříček, V.; Dušek, M.; Palatinus, L. Crystallographic computing system JANA2006: general features. *Z. Kristallogr. - Cryst. Mater.* **2014**, *229*, 345–352.
- (53) Kresse, G.; Furthmüller, J. Efficient iterative schemes for ab initio total-energy calculations using a plane-wave basis set. *Phys. Rev. B: Condens. Matter Mater. Phys.* **1996**, *54*, 11169.
- (54) Kresse, G.; Joubert, D. From ultrasoft pseudopotentials to the projector augmentedwave method. *Phys. Rev. B: Condens. Matter Mater. Phys.* **1999**, *59*, 1758–1775.

(55) Perdew, J. P.; Burke, K.; Ernzerhof, M. Generalized gradient approximation made simple. *Phys. Rev. Lett.* **1996**, *77*, 3865.

(56) Maintz, S.; Deringer, V. L.; Tchougréeff, A. L.; Dronskowski, R. LOBSTER: A tool to extract chemical bonding from plane-wave based DFT. *J. Comput. Chem.* **2016**, *37*, 1030–1035.